Supplementary Information

Zwitterionic nanoparticles for thermally activated drug delivery in hyperthermia cancer treatment

Camillo Colli[a], Ilenia Masi[b], Emanuela Jacchetti[a], Silvia Santoni[a,c], Mattia Sponchioni[a,*], Bianca Maria Colosimo[c], Laura Rosanò[b], Manuela Teresa Raimondi[a], Emanuele Mauri[a,*], Davide Moscatelli[a]

[a]Department of Chemistry, Materials and Chemical Engineering "G. Natta", Politecnico di Milano, piazza L. da Vinci 32, 20133 Milan, Italy

[b]Institute of Molecular Biology and Pathology, National Research Council (CNR), Rome 00185, Italy

[c]Department of Mechanical Engineering, Politecnico di Milano, Via La Masa, 1, 20156, Milan, Italy

*Mattia Sponchioni. Tel.: +39 022399 3197; e-mail: mattia.sponchioni@polimi.it

*Emanuele Mauri. Tel.: +39 022399 3397; e-mail: emanuele.mauri@polimi.it

Synthesis of p(SB-co-ZB)$_{200}$ copolymers

Table S1 reports the amount of reagents involved in the syntheses of the zwitterionic copolymers. GPC of the copolymer p(110SB-co-90ZB), as representative specimens, is showed in Figure S1.

Table S1. Mixture compositions for the synthesis of the different p(SB-co-ZB)$_{200}$ copolymers.

Copolymer	DP$_{SB}$ (-)	DP$_{ZB}$ (-)	SB (mg)	ZB (mg)	ACVA (mg)	CPA (mg)
p(105SB-co-95ZB)	105	95	254	243	0.81	2.42
p(110SB-co-90ZB)	110	90	267	231	0.81	2.42
p(115SB-co-85ZB)	115	85	279	218	0.81	2.42
p(120SB-co-80ZB)	120	80	292	206	0.81	2.42
p(125SB-co-75ZB)	125	75	304	193	0.81	2.42
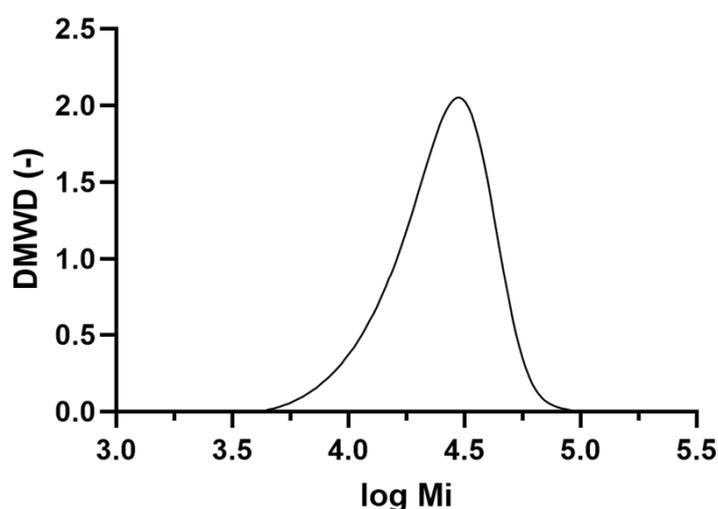
Figure S1. GPC analysis of zwitterionic copolymer p(110SB-co-90ZB).

Paclitaxel calibration curve

The calibration curve of PTX was estimated via HPLC, preparing a stock solution of drug at concentration 1 mg/mL in acetonitrile. The calibration solutions with concentration 500 µg/mL, 100 µg/mL, 10 µg/mL, 5 µg/mL, 1 µg/mL, 0.5 µg/mL, 0.1 µg/mL, 0.05 µg/mL and 0.01 µg/mL were prepared by serial dilutions of the stock solution in acetonitrile. UV-vis measurements were recorded at $\lambda = 230$ nm on a HPLC column (Agilent 1100 System, Agilent Technologies), packed with silica beads and using a mixture of acetonitrile-water 80:20 as a mobile phase.

Calibration curve was obtained by plotting the integral values of the PTX peak vs. drug concentration and using a linear fitting of the experimental data, according to the Lambert-Beer law (Figure S2).
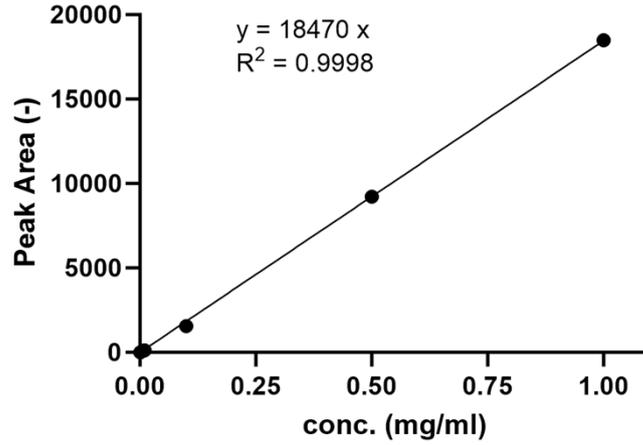
Figure S2. PTX calibration curve in physiological solution (0.9% w/w NaCl)

Dose-response curve of PTX

The dose-response curve of PTX on SKOV3 was evaluated at 24 h, following the hyperthermia treatment (1 h at 43 °C), using the MTT assay. Cells were cultured in adhesion. The value of 1.3 nM was identified as the IC_{50} level and showed by the dashed line in Figure S3.
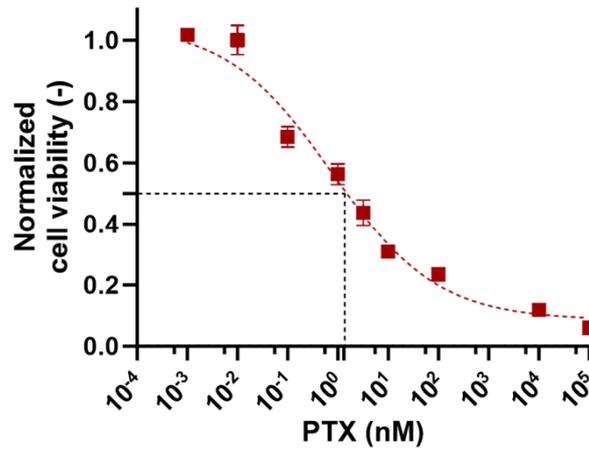
Figure S3. Dose-response curve of PTX. IC_{50} value (black dashed line) of 1.3 nM is highlighted.

UCST behavior of p(SB-co-ZB) copolymers

The synthetized p(SB-co-ZB) copolymers were separately dispersed in physiological solution (5 mg/ml) and the corresponding cloud point was evaluated through UV-Vis spectrophotometric analysis (λ=500 nm), setting a heat-up ramp of 1 °C/min. T_{cp} was identified as the inflection point of the curve transmittance *vs* temperature, corresponding to 50% transmittance (Figure S4).
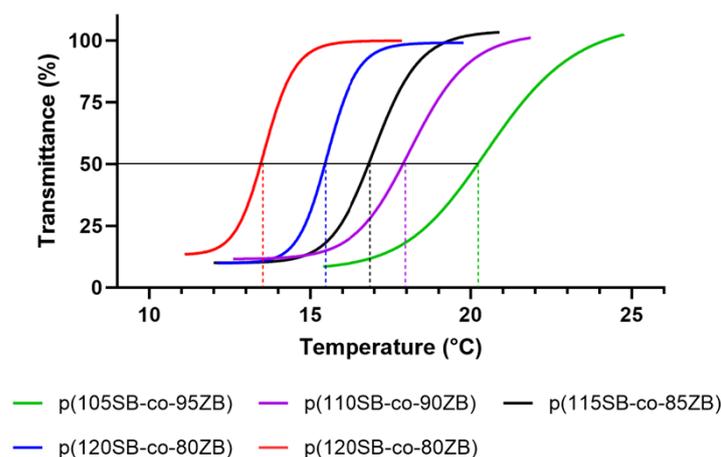
Figure S4. (a) Evaluation of cloud point (T_{cp}) of the synthetized zwitterionic copolymers in graph trasmittance vs temperature, by UV-vis analysis.

IR spectrum of HEMACL$_3$

Figure S5 shows the IR spectrum of HEMACL$_3$. Similarly to HEMACL$_5$, the characteristic peaks of the polymer are highlighted: C-C(=O)-O stretching in the range 1100-1250 cm^{-1} (#), C=O stretching at 1720 cm^{-1} (##), C-H stretching at 2850-3000 cm^{-1} (###) and -OH stretching at 3400 cm^{-1} (####).
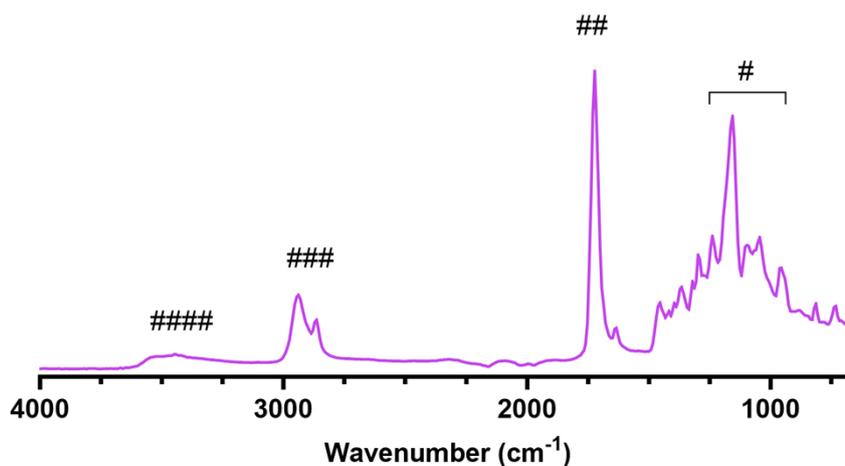
Figure S5. IR spectrum of HEMACL$_3$.

T_cp estimation for UCST-type NPs

The UCST behavior of all synthetized NPs was evaluated through DLS analysis, considering the phase transition as a function of temperature (heat-up ramp of 1 °C/5 min). The average NPs size is reported in Figures S6 for NPs obtained using $HEMACL_5$, and in Figure S7 for NPs containing $HEMACL_3$; the T_{cp} was estimated as inflection point of the hydrodynamic diameter curve. For $HEMACL_5$-based NPs, their thermoresponsiveness after a heating-cooling-heating cycle is reported, showing a narrow hysteresis which suggests the reversible effect of the temperature on the particle size.
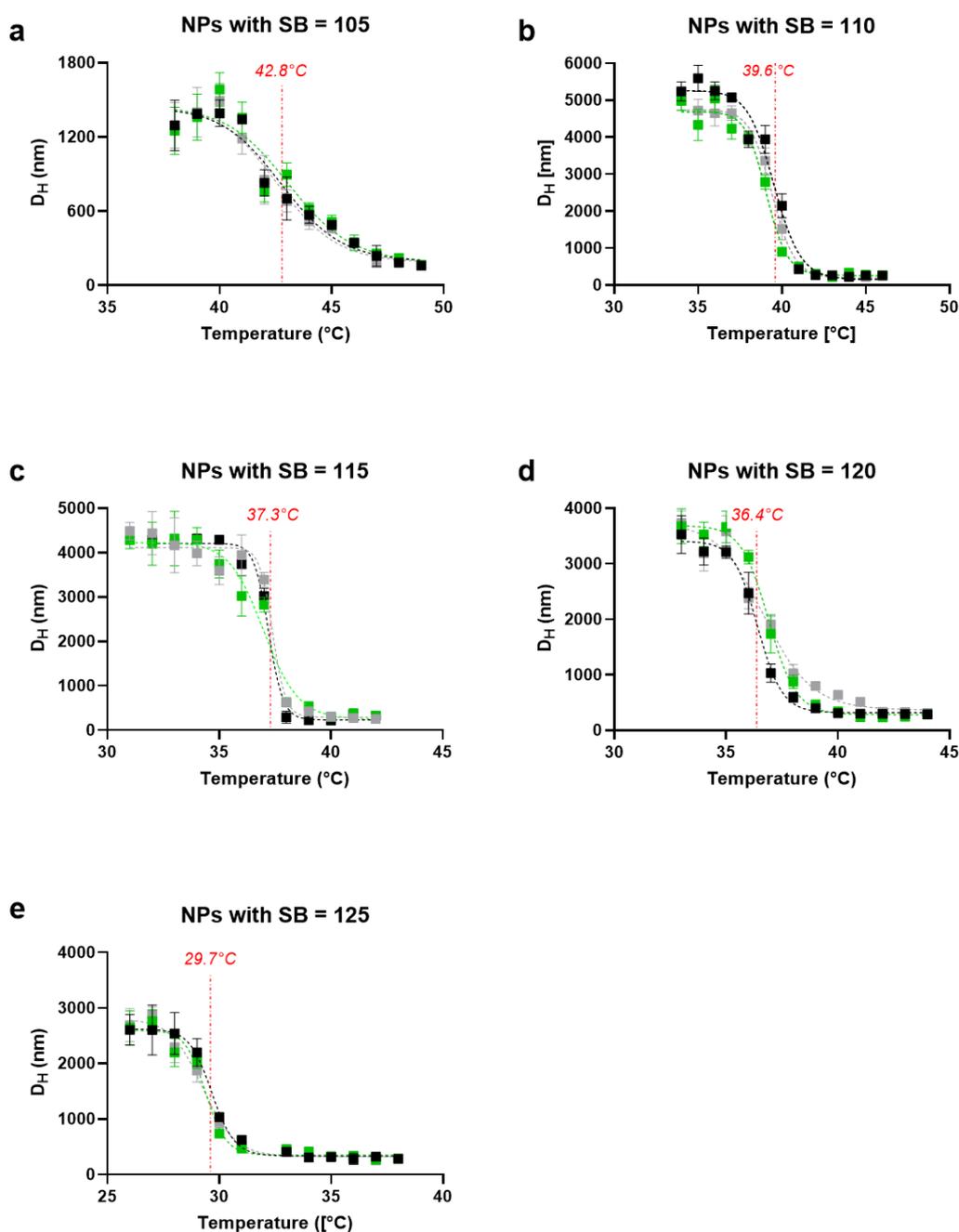
Figure S6. DLS curves of the hydrodynamic diameter of HEMACL$_5$-based NPs as a function of the temperature. The T$_{cp}$ for each specimens is highlighted in red. The heating/cooling cycle is reported as follows: first heating step in black, cooling step in green, and second heating phase in grey. The graphs are labelled according to the zwitterioni copolymer used in the RAFT emulsion polymerization. a: p(105SB-co-95ZB); b: p(115SB-co-85ZB); c: p(120SB-co-80ZB); d: p(125SB-co-75ZB).
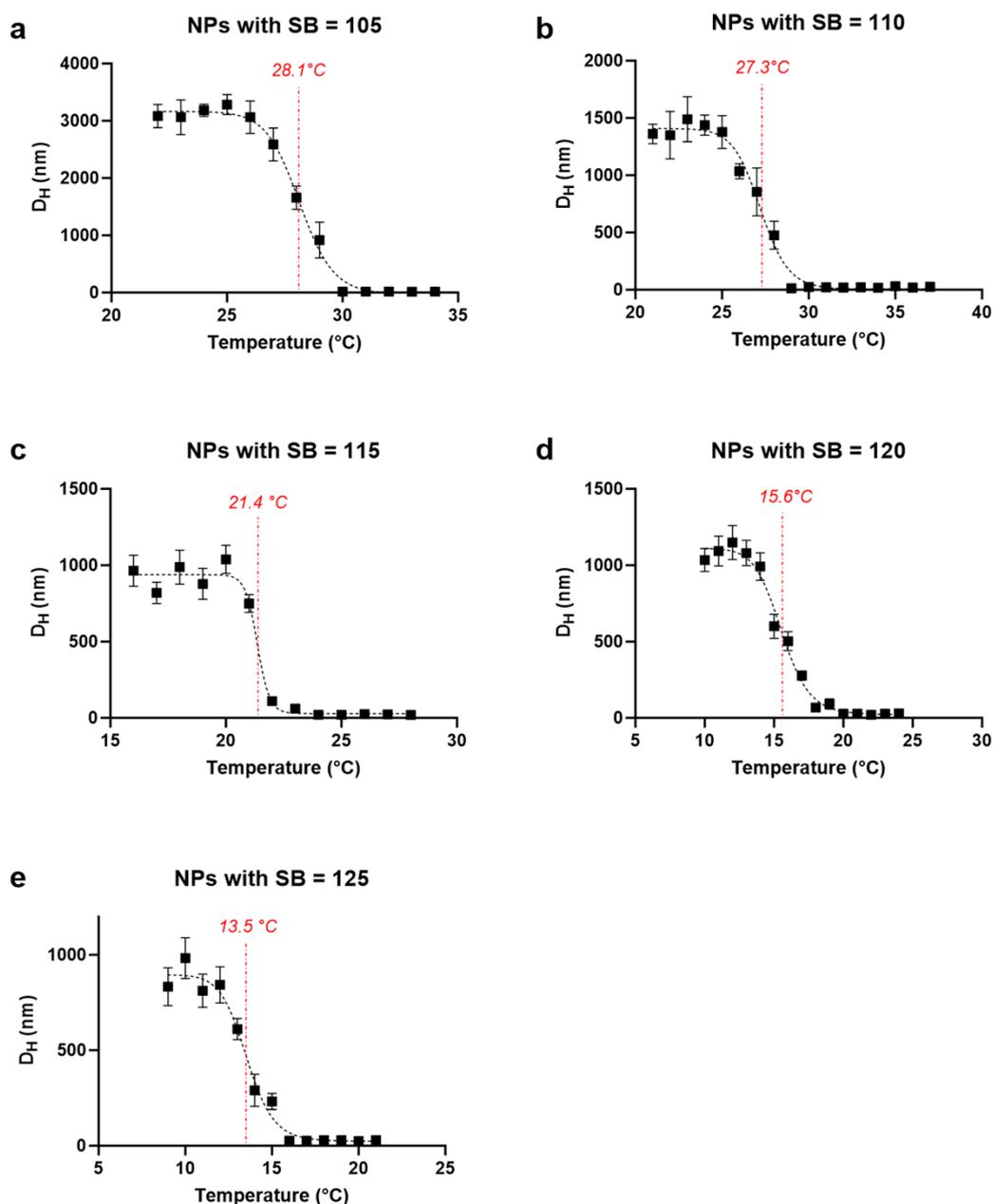
Figure S7. DLS curves of the hydrodynamic diameter of HEMACL$_3$-based NPs as a function of the temperature. The T$_{cp}$ for each specimens is highlighted in red. The graphs are labelled according to the zwitterioni copolymer used in the RAFT emulsion polymerization. a: p(105SB-co-95ZB); b: p(110SB-co-90ZB); c: p(115SB-co-85ZB); d: p(120SB-co-80ZB); e: p(125SB-co-75ZB).

3D rendering of NPs internalization

Figure S8 shows a representative 3D rendering of the confocal z-stack micrographs of NPs internalization in SKOV3 cells after 24 h incubation. Calcein-AM staining confirms that cells preserve their viability.
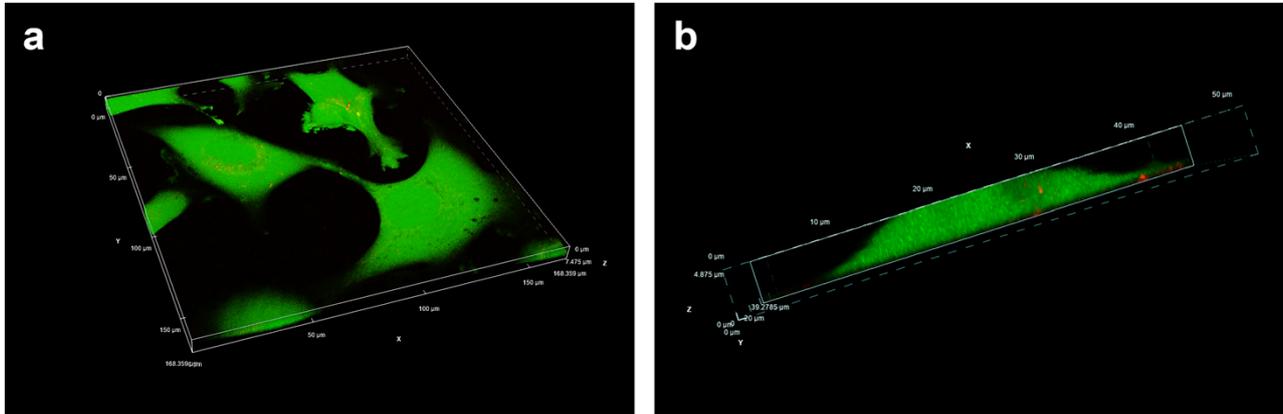
Figure S8. Representative 3D rendering of NPs internalization from confocal z-stack micrographs. In green are visible viable cells stained with Calcein-AM and in red NPs internalized in the cytosol. a) XY cross-sectional view, b) XZ cross-sectional view.